Shipol : a Matlab program for simulation of light-wave propagation in high-power fiber lasers

Stéphane BALAC

UNIV. RENNES, CNRS, IRMAR-UMR 6625, F-35000 Rennes, France

Release 1.1 - June 2021

1 Introduction

In the theoretical study of light-wave propagation in double-clad rare-earth-doped fiber-lasers, the most commonly used mathematical model is based on the rate-equation theory [1, 2] that describes the distributions of inversion populations and optical powers along the fiber when a stationary regime has been attained. In this model, the power propagation equations consist of several coupled non-linear first order ordinary differential equations (ODE) depending on the position z along the fiber [5]. The main difficulty for solving this system of non-linear ODE is related to the boundary conditions. We have a boundary value problem (BVP) and the boundary conditions (BC) for this BVP are not separated, which means that we do not have two independent relations at each endpoint for the unknown but two relations that correlate the values of the unknown function at the two endpoints, see relations (9c) and (9d) in the text below. This mathematical specificity is related to the reflection of the laser signal by Bragg mirrors at the two endpoints. The tricky aspect for numerical simulation is that most of the currently available softwares for BVPs, including MATLAB BVP solvers, assume that the BC are separated, which means that they can not be used in a straightforward way for solving our BVP involved in the simulation of light-wave propagation in high-power fiber lasers.

We have developed an approach that circumvents this issue. It relies in a reformulation of the BVP stemming from the rate-equation theory in an equivalent BVP with separated BC, thereby opening the possibility of using MATLAB BVP solvers. Moreover, since the efficiency of BVP solvers is dependent on the initial guess provided for the solution, it is also important to have or to compute an initial guess close enough to the solution to the BVP. We found that when propagation losses can be neglected, the BVP with non-separated BC can be transformed into an equivalent Initial Value Problem (IVP), for which the solution can be computed simply by using standard ODE solvers such as the one based on Runge-Kutta method (and implemented e.g. in MATLAB `ode45` function). Since losses most often change quite little the general behavior of light-wave propagation in a fiber laser, we have by this way a "good" initial guess for the BVP solver used to solve the more general problem. The two ideas are implemented in the SHIPOL program under MATLAB giving rise to a simple and efficient numerical software for simulation of light-wave propagation in double-clad rare-earth-doped fiber-lasers. The acronym SHIPOL stands for Simulation of HIgh-POwer fiber Lasers.

The document is organized as follows. In Section 2, we introduce the mathematical model for light-wave propagation in high-power fiber-lasers and we detail the way the BVP with non-separated BC classically proposed in the literature can be transformed into an equivalent BVP with separated BC. Then, in Section 3, we explain how to use one of the MATLAB BVP solvers in an efficient way to solve this BVP with separated BC. Namely, we discuss the way an initial guess required by MATLAB BVP solver can be computed so as to be close to the solution for a faster convergence of MATLAB BVP solver and we give the expression of the Jacobian also required by MATLAB BVP solver for a better efficiency. Finally, in Section 4, we present a comprehensive run test to show how to use the SHIPOL program under MATLAB and we carry out a comparison with existing results in the literature for a validation of the SHIPOL program.

2 The mathematical model

We denote by L the length of the fiber and we assume that the axis of the fiber coincides with the z-axis of the reference frame. Using the rate-equation theory under the steady state condition [1, 2], we obtain a set of coupled equations for the pump and laser co-propagative and contra-propagative powers $P_p^+, P_p^-, P_s^+, P_s^-$ describing light-wave propagation in a linear cavity as follows [5]:

$$\begin{cases} \pm\dfrac{\mathrm{d}P_p^{\pm}}{\mathrm{d}z}(z) = \big((\sigma_p^{(e)} + \sigma_p^{(a)})\, N_2(z) - \sigma_p^{(a)} N\big)\, \Gamma_p\, P_p^{\pm}(z) - \alpha_p\, P_p^{\pm}(z) & \text{(1a)} \\ \pm\dfrac{\mathrm{d}P_s^{\pm}}{\mathrm{d}z}(z) = \big((\sigma_s^{(e)} + \sigma_s^{(a)})\, N_2(z) - \sigma_s^{(a)} N\big)\, \Gamma_s\, P_s^{\pm}(z) - \alpha_s\, P_s^{\pm}(z) + \Gamma_s\, \sigma_e^{(s)} P_0\, N_2(z) & \text{(1b)} \end{cases}$$

where

- $P_p^{\pm}$ and $P_s^{\pm}$ represent respectively the pump power (index p) at pump wavelength λ_p and the laser signal power (index s) at laser wavelength λ_s in the forward propagating direction (superscript +) and backward propagating direction (superscript -);
- Γ_p and Γ_s are respectively the overlap integral factors between the ion-doping distribution and mode fields of pump and laser lights;
- $\sigma_p^{(a)}$ and $\sigma_p^{(e)}$ denote respectively the absorption and emission cross-sections at the pump wavelength λ_p;
- $\sigma_s^{(a)}$ and $\sigma_s^{(e)}$ denote respectively the absorption and emission cross-sections at the laser wavelength λ_s;
- α_p and α_s represent the propagation losses coefficients including background loss and scattering loss at the pump and laser wavelengths respectively;
- P_0 represents the contribution to spontaneous emission into the propagation laser mode;
- N is the doping substance concentration density assumed to be constant along the fiber
- N_2 is the upper-level population density of the three levels atomic system underlying the rate equation model.

Note that this model assumes that the pump power is strong enough to saturate the gain [5].

For continuous-wave laser, the upper-level population density N_2 at position z (in unit m^{-3}) is given by [5]:

$$N_2(z) = \frac{\sigma_s^{(a)} \frac{\Gamma_s}{h\nu_s} P_s(z) + \sigma_p^{(a)} \frac{\Gamma_p}{h\nu_p} P_p(z)}{\frac{A_{\text{eff}}}{\tau} + (\sigma_s^{(a)} + \sigma_s^{(e)}) \frac{\Gamma_s}{h\nu_s} P_s(z) + (\sigma_p^{(a)} + \sigma_p^{(e)}) \frac{\Gamma_p}{h\nu_p} P_p(z)}\, N \tag{2}$$

where $P_p(z) = P_p^+(z) + P_p^-(z)$ is the total pump power and $P_s(z) = P_s^+(z) + P_s^-(z)$ is the total laser power, τ is the spontaneous emission lifetime, A_{eff} is the effective doping area, $h = 6.62607015\, 10^{-34}\ \mathrm{J \cdot s}$ is the Planck's constant and $\nu_p = \frac{c}{\lambda_p}$, $\nu_s = \frac{c}{\lambda_s}$, where $c = 299\,792\,458\ \mathrm{m \cdot s^{-1}}$ denotes light velocity in vacuum, are respectively the pump and laser frequencies.

We define the pump attenuation constant $\alpha_p^{(a)}$ and the laser attenuation constant $\alpha_s^{(a)}$ (both in unit m^{-1}) as

$$\alpha_p^{(a)} = N\ \Gamma_p\ \sigma_p^{(a)} \tag{3a}$$
$$\alpha_s^{(a)} = N\ \Gamma_s\ \sigma_s^{(a)} \tag{3b}$$

and the saturation powers for the pump and laser (in unit W) as

$$P_p^{\text{sat}} = \frac{A_{\text{eff}} h\nu_p}{\tau\, (\sigma_p^{(a)} + \sigma_p^{(e)})\, \Gamma_p} \tag{4a}$$
$$P_s^{\text{sat}} = \frac{A_{\text{eff}} h\nu_s}{\tau\, (\sigma_s^{(a)} + \sigma_s^{(e)})\, \Gamma_s} \tag{4b}$$

Using the above defined quantities, the ion population density N_2 given by (2) can be expressed as

$$N_2(z) = \frac{\tau}{A_{\text{eff}}} \frac{\frac{\alpha_p^{(a)}}{h\nu_p} P_p(z) + \frac{\alpha_s^{(a)}}{h\nu_s} P_s(z)}{1 + \frac{P_s(z)}{P_s^{\text{sat}}} + \frac{P_p(z)}{P_p^{\text{sat}}}} \tag{5}$$

Substituting N_2 as given by (5) into the propagation equations (1), we obtain the following non-linear system of ODE

$$\begin{cases} \pm \dfrac{\mathrm{d}P_p^{\pm}}{\mathrm{d}z}(z) = -\left(\alpha_p^{(a)} + \alpha_p\right) P_p^{\pm}(z) + G_p(P_p^{\pm}(z), P_s^{\pm}(z)) \dfrac{P_p^{\pm}(z)}{P_p^{\text{sat}}} & \text{(6a)} \\ \pm \dfrac{\mathrm{d}P_s^{\pm}}{\mathrm{d}z}(z) = -\left(\alpha_s^{(a)} + \alpha_s\right) P_s^{\pm}(z) + G_s(P_p^{\pm}(z), P_s^{\pm}(z)) \left(\dfrac{P_s^{\pm}(z)}{P_s^{\text{sat}}} + \dfrac{P_0}{P_s^{\text{sat},e}} \right) & \text{(6b)} \end{cases}$$

where (we recall that $P_p = P_p^+ + P_p^-$ and $P_s = P_s^+ + P_s^-$)

$$G_p(P_p^{\pm}(z), P_s^{\pm}(z)) = \frac{\alpha_p^{(a)} P_p(z) + \frac{\nu_p}{\nu_s}\alpha_s^{(a)} P_s(z)}{1 + \frac{P_s(z)}{P_s^{\text{sat}}} + \frac{P_p(z)}{P_p^{\text{sat}}}} \tag{7a}$$

$$G_s(P_p^{\pm}(z), P_s^{\pm}(z)) = \frac{\alpha_s^{(a)} P_s(z) + \frac{\nu_s}{\nu_p}\alpha_p^{(a)} P_p(z)}{1 + \frac{P_s(z)}{P_s^{\text{sat}}} + \frac{P_p(z)}{P_p^{\text{sat}}}} \tag{7b}$$

and where, with reference to (4b), we have set

$$P_s^{\text{sat},e} = \frac{A_{\text{eff}} h\nu_s}{\tau\, \sigma_s^{(e)}\, \Gamma_s} \tag{8}$$

The boundary conditions (BC) are as follows [5]:

$$\begin{cases} P_p^+(0) = R_p^{(1)} P_p^-(0) + P_{\text{pump}}^+ & \text{(9a)} \\ P_p^-(L) = R_p^{(2)} P_p^+(L) + P_{\text{pump}}^- & \text{(9b)} \\ P_s^+(0) = R_s^{(1)}\, P_s^-(0) & \text{(9c)} \\ P_s^-(L) = R_s^{(2)}\, P_s^+(L) & \text{(9d)} \end{cases}$$

where P_{pump}^+ and P_{pump}^- are the launched pump powers into the front ($z = 0$) and back ($z = L$) ends respectively, $R_s^{(1)}$ and $R_s^{(2)}$ are the reflectivities of the laser cavity at the front and back ends, respectively at the laser source wavelength λ_s and $R_p^{(1)}$ and $R_p^{(2)}$ are the reflectivities at the pump wavelength λ_p.

Thus, we have to solve a BVP that consists of the non-linear first order coupled ODE (6) and the linear two-point BC (9). The specificity of these BC is that they are not separated due to reflections at the fiber ends that mix forward and backward propagating powers. Unfortunately, most of the currently available softwares for BVPs, including MATLAB BVP solvers, assumes that the BC are separated. Therefore, it is not possible to solve directly BVP (6)–(9) using existing softwares such as MATLAB. Let's put aside the unnecessarily complicated numerical approaches published in [7, 11, 3, 4] and let us apply to BVP (6)–(9) a tricks that can transform it into a BVP with separated BC.

We can express BVP (6)–(9) in the form

$$Y'(z) = F(Y(z)) \qquad \forall z \in]0, L[\tag{10}$$

where the unknown vector $Y(z) \in \mathbb{R}^4$ is defined as $Y(z) = \left(P_p^+(z), P_p^-(z), P_s^+(z), P_s^-(z)\right)^\top$ where $^\top$ indicates matrix/vector transposition and the mapping F is defined as

$$F : Y \in \mathbb{R}^4 \longmapsto \begin{pmatrix} -(\alpha_p^{(a)} + \alpha_p)\, Y_1 + G_p(Y)\, \frac{Y_1}{P_p^{\text{sat}}} \\ (\alpha_p^{(a)} + \alpha_p)\, Y_2 - G_p(Y)\, \frac{Y_2}{P_p^{\text{sat}}} \\ -(\alpha_s^{(a)} + \alpha_s)\, Y_3 + G_s(Y) \left(\frac{Y_3}{P_s^{\text{sat}}} + \frac{P_0}{P_s^{\text{sat},e}} \right) \\ (\alpha_s^{(a)} + \alpha_s)\, Y_4 - G_s(Y) \left(\frac{Y_4}{P_s^{\text{sat}}} + \frac{P_0}{P_s^{\text{sat},e}} \right) \end{pmatrix} \tag{11}$$

where here and throughout the paper $Y_1, \ldots, Y_4$ denotes the components of Y. The BC (9) can be expressed in matrix form as

$$\mathrm{M}_0\, Y(0) + \mathrm{M}_L\, Y(L) = \begin{pmatrix} P^+_{\mathrm{pump}} \\ P^-_{\mathrm{pump}} \\ 0 \\ 0 \end{pmatrix} \tag{12}$$

where the two matrices M_0 and M_L in $\mathcal{M}_4(\mathbb{R})$ are given by

$$\mathrm{M}_0 = \begin{pmatrix} 1 & -R_p^{(1)} & 0 & 0 \\ 0 & 0 & 0 & 0 \\ 0 & 0 & 1 & -R_s^{(1)} \\ 0 & 0 & 0 & 0 \end{pmatrix} \qquad \mathrm{M}_L = \begin{pmatrix} 0 & 0 & 0 & 0 \\ -R_p^{(2)} & 1 & 0 & 0 \\ 0 & 0 & 0 & 0 \\ 0 & 0 & -R_s^{(2)} & 1 \end{pmatrix}$$

The BVP (10) – (12) can be solved using one of the MATLAB BVP solvers and the first fourth components of U give the sought out powers $P_p^{\pm}$ and $P_s^{\pm}$.

3 The SHIPOL program

3.1 Use of MATLAB BVP solvers in the SHIPOL program

MATLAB BVP solver `bvp4c` implements a collocation method based on the three-stage Lobatto IIIa formula to solve BVP with separated BC, see [6]. MATLAB BVP solver `bvp5c` implements the four-stage Lobatto IIIa formula and slightly differs from `bvp4c` on some internal implementation choices, see MATLAB documentation for details [8]. MATLAB BVP solvers efficiency is improved when

1. an initial guess close enough to the solution is provided
2. the Jacobian matrix of the function F defining the ODE is available.

We examine now these two topics for BVP (10) with BC (12). (Or equivalently for BVP (6) with BC (9).)

3.1.1 Computation of the initial guess

Propagation losses in the fiber, although not negligible, are generally small and they contribute lowly to the BVP solution that is mainly driven by other optical phenomena. The same can be observed concerning the contribution to spontaneous emission into the propagation laser mode. These observations lead us to chose as initial guess for MATLAB BVP solvers, the solution to BVP (10) in the case when $\alpha_p = \alpha_s = 0$ and $P_0 = 0$. This idea would be idiotic if solving the BVP under these assumptions was as difficult as solving the complete BVP, but such is not the case. Indeed, we show in Appendix A p. 14 that when losses and spontaneous emission are neglected, BVP (6)–(9) can be reformulated in an equivalent Initial Value Problem (IVP) easy to solve by a numerical method. This IVP is composed of the same ODE system (6) as the BVP considered with $\alpha_p = \alpha_s = 0$ and $P_0 = 0$, that is to say the ODE system is

$$\begin{cases} \pm \dfrac{\mathrm{d}P_p^{\pm}}{\mathrm{d}z}(z) = -\,\alpha_p^{(a)}\, P_p^{\pm}(z) + G_p(P_p^{\pm}(z), P_s^{\pm}(z))\, \dfrac{P_p^{\pm}(z)}{P_p^{\mathrm{sat}}} & \text{(13a)} \\ \pm \dfrac{\mathrm{d}P_s^{\pm}}{\mathrm{d}z}(z) = -\,\alpha_s^{(a)}\, P_s^{\pm}(z) + G_s(P_p^{\pm}(z), P_s^{\pm}(z))\, \dfrac{P_s^{\pm}(z)}{P_s^{\mathrm{sat}}} & \text{(13b)} \end{cases}$$

where the mapping G_s and G_p are defined in (7). As shown in Appendix A, the Initial conditions are

$$P_p^-(0) = \frac{P_{\text{pump}}^+ R_p^{(2)} + P_{\text{pump}}^- \, \mathrm{e}^A}{\mathrm{e}^{2A} - R_p^{(1)} R_p^{(2)}} \tag{14a}$$

$$P_s^-(0) = \frac{P_s^{\text{sat}}}{B}\left(\frac{1}{2}\log(R_s^{(1)} R_s^{(2)}) - \frac{\nu_s}{\nu_p}\frac{1}{P_s^{\text{sat}}} C - \alpha_s^a L\right) \tag{14b}$$

$$P_p^+(0) = R_p^{(1)} P_p^-(0) + P_{\text{pump}}^+ \tag{14c}$$

$$P_s^+(0) = R_s^{(1)} \, P_s^-(0) \tag{14d}$$

where

$$A = \frac{\nu_p P_s^{\text{sat}}}{\nu_s P_p^{\text{sat}}}\left(\frac{1}{2}\log(R_s^{(1)} R_s^{(2)}) - \alpha_s^a L\right) + \alpha_p^a L$$

$$B = \sqrt{R_s^{(1)}/R_s^{(2)}} - R_s^{(1)} - \sqrt{R_s^{(1)} R_s^{(2)}} + 1$$

$$C = (1 - R_p^{(2)})D + (1 - R_p^{(1)})P_p^-(0) - (P_{\text{pump}}^+ + P_{\text{pump}}^-)$$

$$D = \sqrt{\left(\frac{P_{\text{pump}}^-}{2R_p^{(2)}}\right)^2 + \frac{R_p^{(1)}}{R_p^{(2)}}\left(P_p^-(0)\right)^2 + \frac{P_{\text{pump}}^-}{R_p^{(2)}} P_p^-(0) - \frac{P_{\text{pump}}^-}{2R_p^{(2)}}}$$

Note that these initial conditions are fully determined provided they are computed in the following order : A, $P_p^-(0)$, $P_p^+(0)$, B, D, C, $P_s^-(0)$ and $P_s^+(0)$.

The IVP (13)–(14) can be solved easily using e.g. the Runge-Kutta method implemented in MATLAB `ode45` solver [10]. The solution $Y : z \in [0, L] \mapsto \left(P_p^+(z), P_p^-(z), P_s^+(z), P_s^-(z)\right)^\top \in \mathbb{R}^4$ though different from the real solution to the BVP is likely to be close to it and it will thus provide a very good initial guess for MATLAB BVP solvers. Denoting by Y_j the solution to this IVP at grid node z_j of a subdivision $(z_j)_{j=0,\dots,J}$ of the interval $[0, L]$, we provide to MATLAB BVP solver `bvp4c` as initial guess $Y_0 = \left(P_p^+(0), P_p^-(0), P_s^+(0), P_s^-(0)\right)^\top$ given by (14).

3.1.2 Computation of the Jacobian matrix of the mapping F

Let us now consider the calculation of the Jacobian matrix J_F of the mapping F introduced in (10). A straightforward calculation shows that the partial derivatives of F are given for $j \in \{1, \dots, 4\}$ and for $Y \in \mathbb{R}^4$ by

$$\partial_j F_1(Y) = -(\alpha_p^{(a)} + \alpha_p)\,\delta_{1,j} + \frac{G_p(Y)}{P_p^{\text{sat}}}\,\delta_{1,j} + \frac{Y_1}{P_p^{\text{sat}}}\,\partial_j G_p(Y) \tag{15a}$$

$$\partial_j F_2(Y) = (\alpha_p^{(a)} + \alpha_p)\,\delta_{2,j} - \frac{G_p(Y)}{P_p^{\text{sat}}}\,\delta_{2,j} - \frac{Y_2}{P_p^{\text{sat}}}\,\partial_j G_p(Y) \tag{15b}$$

$$\partial_j F_3(Y) = -(\alpha_s^{(a)} + \alpha_s)\,\delta_{3,j} + \frac{G_s(Y)}{P_s^{\text{sat}}}\,\delta_{3,j} + \left(\frac{Y_3}{P_s^{\text{sat}}} + \frac{P_0}{P_s^{\text{sat},e}}\right)\partial_j G_s(Y) \tag{15c}$$

$$\partial_j F_4(Y) = (\alpha_s^{(a)} + \alpha_s)\,\delta_{4,j} - \frac{G_s(Y)}{P_s^{\text{sat}}}\,\delta_{4,j} - \left(\frac{Y_4}{P_s^{\text{sat}}} + \frac{P_0}{P_s^{\text{sat},e}}\right)\partial_j G_s(Y) \tag{15d}$$

where $\delta_{i,j}$ denotes the Kronecker symbol (equal to 1 when $i = j$ and 0 otherwise) and ∂_j refers to the partial derivation with respect to the j-th variable. The partial derivatives of the mappings G_p and G_s defined in (7) are given by

$$\partial_1 G_p(Y) = \partial_2 G_p(Y) = \left(\alpha_p^{(a)} - \frac{G_p(Y)}{P_p^{\text{sat}}}\right)\psi(Y)$$

$$\partial_3 G_p(Y) = \partial_4 G_p(Y) = \left(\frac{\nu_p}{\nu_s}\,\alpha_s^{(a)} - \frac{G_p(Y)}{P_s^{\text{sat}}}\right)\psi(Y)$$

and

$$\partial_1 G_s(Y) = \partial_2 G_s(Y) = \Big(\frac{\nu_s}{\nu_p}\,\alpha_p^{(a)} - \frac{G_s(Y)}{P_p^{\rm sat}}\Big)\,\psi(Y)$$
$$\partial_3 G_s(Y) = \partial_4 G_s(Y) = \Big(\alpha_s^{(a)} - \frac{G_s(Y)}{P_s^{\rm sat}}\Big)\,\psi(Y)$$

where $\psi(Y) = 1 + \dfrac{Y_1+Y_2}{P_p^{\rm sat}} + \dfrac{Y_3+Y_4}{P_s^{\rm sat}}$.

3.2 Algorithm implemented in SHIPOL program

The algorithm implemented in the SHIPOL program basically consists in the following stages :

1. Computation of a guess by solving ODE (6) with $\alpha_s = \alpha_p = P_0 = 0$ under the initial conditions given by (14) for $P_p^{\pm}(0)$ and $P_s^{\pm}(0)$ using MATLAB `ode45` solver.
2. Solving of the BVP (10) with separated BC (12) by MATLAB `bvp4c` solver starting from the guess computed at stage 1. Efficiency of `bvp4c` is improved when the Jacobian matrix of F is provided.
3. Plotting of the results. The values of the pump and laser co-propagative and contra-propagative powers $P_p^{\pm}, P_s^{\pm}$ along the fiber length $[0, L]$ are depicted together with the variation of the ratio $N_2(z)/N$ given by relation (2) for $z \in [0, L]$.

Note that the accuracy of the computed solution can be evaluated using an error estimator based on the relations $P_p^+(0)\,P_p^-(0) = P_p^+(L)\,P_p^-(L)$ and $P_s^+(0)\,P_s^-(0) = P_s^+(L)\,P_s^-(L)$ (this latter is valid only when $P_0 = 0$) as stated in the Appendix, see relation (A.17). Therefore, we use as error estimator the quantities $\mathfrak{E}_p$ and $\mathfrak{E}_s$ defined as

$$\mathfrak{E}_P = \left|\frac{P_p^+(0)\,P_p^-(0) - P_p^+(L)\,P_p^-(L)}{P_p^+(0)\,P_p^-(0) + P_p^+(L)\,P_p^-(L)}\right| \tag{16a}$$
$$\mathfrak{E}_s = \left|\frac{P_s^+(0)\,P_s^-(0) - P_s^+(L)\,P_s^-(L)}{P_s^+(0)\,P_s^-(0) + P_s^+(L)\,P_s^-(L)}\right| \tag{16b}$$

Note that $\mathfrak{E}_s$ is relevant only when $P_0 \equiv 0$. The closer to zero these estimators are, the more accurate the computation can be expected to be.

The SHIPOL program is compound of the following MATLAB files :

- `shipol.m` : main MATLAB file implementing the three steps of the algorithm described above;
- `jacF.m` : provides the Jacobian matrix of the mapping F defining the BVP, see (11) and (15).

In addition, a third MATLAB file is used to provide the features of the fiber-laser under investigation in a specific format, see Section 4.1 for details.

4 Numerical illustrations

4.1 A comprehensive run test

We consider simulation of light-wave propagation in a Yb^{3+} doped fiber-laser using SHIPOL program run under MATLAB. We use the Yb^{3+}-doped fiber-laser investigated in [5], the parameters of which are given in Table 1. The results presented here were obtained using MATLAB R2018b running under Linux-Ubuntu OS on an Intel Core i5 laptop computer with 8 Go RAM.

The first step when using the SHIPOL program is to provide the features of the fiber-laser under investigation in a auxiliary data file to be included in the SHIPOL program. This data file must have

Parameter	Notation	Value
Fiber length	L	$50\,\mathrm{m}$
Pump wavelength	λ_p	$9.2\,10^{-7}\,\mathrm{m}$
Signal wavelength	λ_s	$1.09\,10^{-6}\,\mathrm{m}$
Pump power at front end	P^{+}_{pump}	$20\,\mathrm{W}$
Pump power at the back end	P^{-}_{pump}	$0\,\mathrm{W}$
Pump overlap factor	Γ_p	$1.2\,10^{-3}$
Signal overlap factor	Γ_s	$8.2\,10^{-1}$
Doping substance concentration	N_t	$4\,10^{25}\,\mathrm{ions/m^3}$
Pump absorption cross section	$\sigma_p^{(a)}$	$6\,10^{-25}\,\mathrm{m^2}$
Pump emission cross section	$\sigma_p^{(e)}$	$2.5\,10^{-26}\,\mathrm{m^2}$
Signal absorption cross section	$\sigma_s^{(a)}$	$1.4\,10^{-27}\,\mathrm{m^2}$
Signal emission cross section	$\sigma_s^{(e)}$	$2\,10^{-25}\,\mathrm{m^2}$
Pump background losses	α_p	$3\,10^{-3}\,\mathrm{m^{-1}}$
Signal background losses	α_s	$5\,10^{-3}\,\mathrm{m^{-1}}$
Front mirror reflectivity	$R_s^{(1)}$	0.98
Output mirror reflectivity	$R_s^{(2)}$	0.04
Lifetime of the upper-level atoms	τ	$10^{-3}\,\mathrm{s}$
Effective mode area	A_{eff}	$5\,10^{-11}\,\mathrm{m}$
Contribution of the spontaneous emission	P_0	$0\,\mathrm{W}$

Table 1: Parameter values for the Yb^{3+} doped fiber-laser investigated in [5].

the following form and must contains the following variables initialized according to the features of the fiber-laser. The example provided below is for the Yb^{3+} doped fiber-laser investigated in [5] with its parameter values given in Table 1. Note that it is of the upmost importance to use the unit of the SI system as indicated in this sample data file and in Table 1. The name of the variable for each of the parameter describing the fiber-laser must also be keep as indicated in this sample data file (provided in the SHIPOL archive).

```
% Description of the fiber
Nt= 4E25;   % Doping substance concentration [ions/m^3]
tau3= 1E-3;   % Lifetime of the upper-level atoms [s]
Aeff=5E-11;% Effective mode area [m^2]
L=50; % fiber length [m]

% Description of the pump
sigma_a_p= 6E-25  ; % pump absorption cross section [m^2]
sigma_e_p= 2.5E-26 ;     %  pump emission cross section [m^2]
alpha_p= 3E-3;    % Pump background losses [m^-1]
Gamma_p= 0.0012;    % Pump overlap factor
lambda_p= 0.92E-6;  % Pump wavelength [m]
Ppump_p=20; % launch Pump Power at z=0  P^+_p(0)  [W]
Ppump_m=0;  % launch Pump Power at z=L   P^-_p(L) [W]
R1_p=0; % front mirror reflexivity at pump wavelength  [dimensionless quantity]
R2_p=0; % output mirror reflexivity  at pump wavelength [dimensionless quantity]

% description of the laser signal
sigma_a_s= 1.4E-27;  % Laser signal absorption cross section [m^2]
sigma_e_s= 2E-25; % Laser signal emission cross section [m^2]
alpha_s= 5E-3;      % Laser signal Pump background losses [m^-1]
Gamma_s=0.8;      % Laser signal overlap factor  [dimensionless quantity]
lambda_s= 1.09E-6;  % Laser signal wavelength [m]
R1_s=0.98; % front mirror reflexivity at laser signal wavelength  [dimensionless quantity]
R2_s=0.04; % output mirror reflexivity  at laser signal wavelength  [dimensionless quantity]
```

```
% contribution of the spontaneous emission into the propagating laser mode
P0=0; % [W]
```

Assuming that the above data have been recorded in a file named `data_yb.m` (this file is provided in the SHIPOL archive), the SHIPOL program runs as follows under MATLAB:

```
>> shipol
[?] Name of the fiber parameters data file : data_yb.m

Done! Overall simulation CPU time = 1.67 s.

Forward pump power at z=0 :   P^+_p(0) = 20 W
Backward pump power at z=0 :  P^-_p(0) = 0 W
Forward laser power at z=0 :  P^+_s(0) = 2.02871 W
Backward laser power at z=0 : P^-_s(0) = 2.07011 W
Forward pump power at z=L :   P^+_p(L) = 4.15728 W
Backward pump power at z=L :  P^-_p(L) = 0 W
Forward laser power at z=L :  P^+_s(L) = 10.2465 W
Backward laser power at z=L : P^-_s(L) = 0.409861 W

Theoretical available power at 920 nm : 13.3718 W
Total laser output power (at z=0 and z=L) : 9.87807 W

Error estimator E_s = 2.7418e-12
```

Note that the program execution time is very short : The CPU time for the simulation was less than 2 s. The error estimator defined in (16b) is found to be $\mathfrak{E}_s = 2.7418\,10^{-12}$. (Note that the estimator $\mathfrak{E}_p$ is not relevant here since $P_s^- \equiv 0$.) We obtain a forward laser power at $z = 0$ with value $P_s^+(0) = 2.02871$ W and a backward laser power at $z = 0$ with value $P_s^-(0) = 2.07011$W. At the fiber back end $z = L$, the values are $P_s^+(L) = 10.2465$ W and $P_s^-(L) = 0.409861$ W. The forward pump power at $z = L$ is 4.15728 W whereas the backward pump power remains zero along the fiber.

The SHIPOL program also provides a graphical representation of the pump and laser powers in the forward and backward directions, *i.e.* $P_p^{\pm}, P_s^{\pm}$, as a function of the position along the fiber with a scale on the left-axis together with the ratio $N_2(z)/N$ with a scale on the right-axis. The result is depicted in Fig. 1. This figure is identical to the one depicted in [5, Fig. 8]. Note that the numerical method used in [5] to solve the BVP is not specified in the paper.

4.2 Code validation by comparison with existing results in the literature

4.2.1 Simulation of light-wave propagation in a Nd^{3+} doped fiber-laser

We have compared the results provided by the SHIPOL program to the ones given in [5] for a Nd^{3+}-doped high-power double-clad fiber laser characterized by the parameters given in Table 2. We have depicted in Fig. 2a the pump and laser powers in the forward and backward directions, *i.e.* $P_p^{\pm}, P_s^{\pm}$, provided by the SHIPOL program as a function of the position along the fiber together with the ratio $N_2(z)/N$. This figure is identical to the one depicted in [5, Fig. 5]. We have obtained a forward laser power at $z = 0$ with value $P_s^+(0) = 2.50126$ W and a backward laser power at $z = 0$ with value $P_s^-(0) = 2.5523$ W. At the fiber back end $z = L$, the values are $P_s^+(L) = 12.6333$ W and $P_s^-(L) = 0.505331$ W. The forward pump power at $z = L$ is 2.19664 W whereas the backward pump power remains zero along the fiber. The CPU time for the simulation was 0.6 s and the error estimator defined in (16b) was $\mathfrak{E}_s = 2.6426\,10^{-12}$. (Note that the estimator $\mathfrak{E}_p$ is not relevant here since $P_s^- \equiv 0$.)

For comprehensiveness, we have also made a simulation when the pump is injected at the fiber back end $z = L$, *i.e.* $P_p^+(0) = 0$ and $P_p^-(L) = 20$W, the other parameters are as given in Table 2. The result is depicted in Fig. 2b and it is identical to the one depicted in [5, Fig. 6].

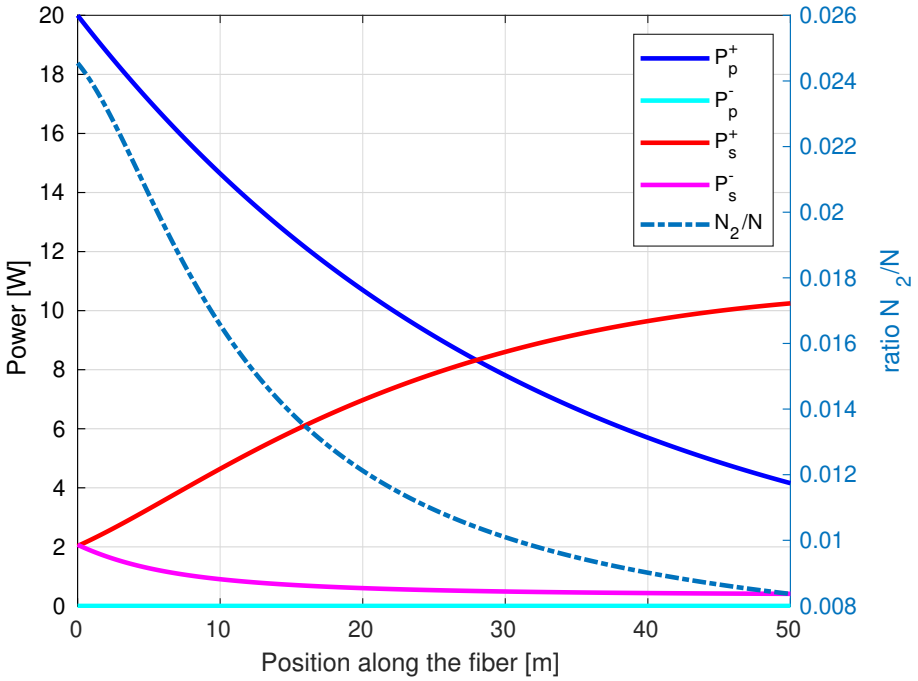

Figure 1: Pump and laser powers in the forward and backward directions $P_p^+, P_p^-, P_s^+, P_s^-$ as a function of the position along the fiber for the Yb^{3+} fiber-laser the parameters of which are given in Table 1 (left axis). Ratio $N_2(z)/N$ as a function of the position along the fiber in dotted line (right axis).

Parameter	Notation	Value
Fiber length	L	$50\,\mathrm{m}$
Pump wavelength	λ_p	$0.808\,10^{-6}\,\mathrm{m}$
Signal wavelength	λ_s	$1.060\,10^{-6}\,\mathrm{m}$
Pump power at front end	P^+_{pump}	$20\,\mathrm{W}$
Pump power at back end	P^-_{pump}	$0\,\mathrm{W}$
Pump overlap factor	Γ_p	0.01
Signal overlap factor	Γ_s	0.8
Doping substance concentration	N_t	$2\,10^{24}\,\mathrm{ions/m^3}$
Pump absorption cross section	$\sigma_p^{(a)}$	$2\,10^{-24}\,\mathrm{m^2}$
Pump emission cross section	$\sigma_p^{(e)}$	$0\,\mathrm{m^2}$
Signal absorption cross section	$\sigma_s^{(a)}$	$0\,\mathrm{m^2}$
Signal emission cross section	$\sigma_s^{(e)}$	$2.5\,10^{-24}\,\mathrm{m^2}$
Pump background losses	α_p	$4.5\,10^{-3}\,\mathrm{m^{-1}}$
Signal background losses	α_s	$0\,\mathrm{m^{-1}}$
Front mirror reflectivity	$R_s^{(1)}$	0.98
Output mirror reflectivity	$R_s^{(2)}$	0.04
Lifetime of the upper-level atoms	τ	$4\,10^{-4}\,\mathrm{s}$
Effective mode area	A_{eff}	$1\,10^{-11}\,\mathrm{m}$
Contribution of the spontaneous emission	P_0	$0\,\mathrm{W}$

Table 2: Parameter values for the Nd^{3+} doped fiber-laser tested in [5].

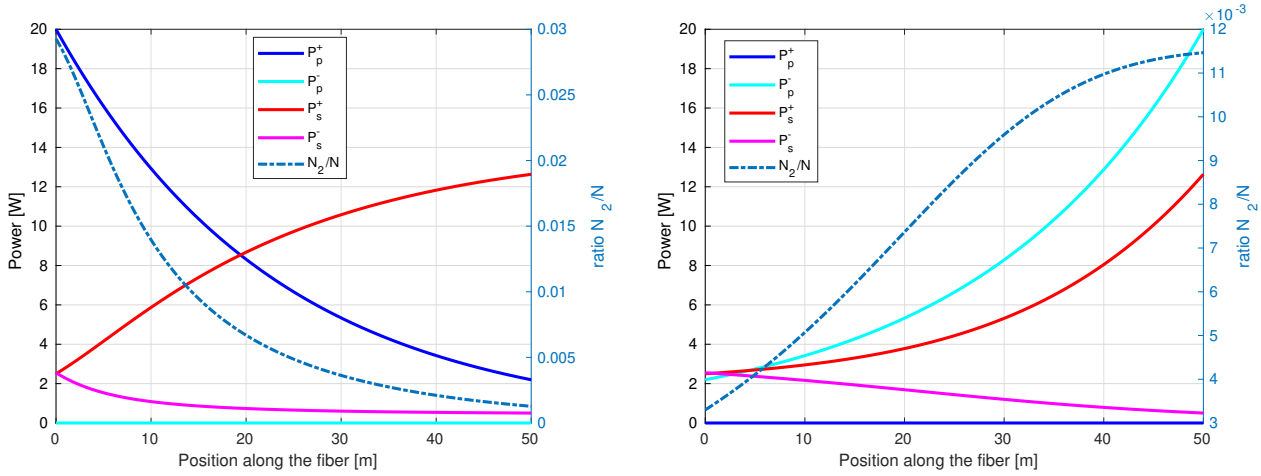

(a) Pump injected at $z = 0$.

(b) Pump injected at $z = L$.

Figure 2: Pump and laser powers in the forward and backward directions $P_p^{\pm}, P_s^{\pm}$ as a function of the position along the fiber for the Nd^{3+} fiber-laser, the parameters of which are given in Table 2, when the pump power is injected at front end (Fig. a), *i.e.* $P^{+}_{\text{pump}} = 20\,\text{W}$ and when the pump power is injected at back end (Fig. b), *i.e.* $P^{-}_{\text{pump}} = 20\,\text{W}$ (values given on the left axis). Ratio $N_2(z)/N$ as a function of the position along the fiber in dotted line and right axis.

4.2.2 Simulation of light-wave propagation in a thulium-doped fiber-laser

Finally, we have considered the case of a Tm^{3+}-doped high-power double-clad fiber-laser proposed in [7] characterized by the values given in Table 3. Note that the doping substance concentration given in [7] was $N = 4.68\,10^{26}\,\text{ions/m}^3$ and it is changed for $N = 8.6\,10^{25}\,\text{ions/m}^3$ to comply with the value of the literature quoted in [7].

Parameter	Notation	Value
Fiber length	L	$25\,\text{m}$
Pump wavelength	λ_p	$0.790\,10^{-6}\,\text{m}$
Signal wavelength	λ_s	$1.973\,10^{-6}\,\text{m}$
Pump power at front end	P^+_{pump}	$1000\,\text{W}$
Pump power at back end	P^-_{pump}	$0\,\text{W}$
Pump overlap factor	Γ_p	0.01
Signal overlap factor	Γ_s	0.752
Doping substance concentration	N_t	$8.6\,10^{25}\,\text{ions/m}^3$
Pump absorption cross section	$\sigma_p^{(a)}$	$5\,10^{-25}\,\text{m}^2$
Pump emission cross section	$\sigma_p^{(e)}$	$0\,\text{m}^2$
Signal absorption cross section	$\sigma_s^{(a)}$	$1\,10^{-26}\,\text{m}^2$
Signal emission cross section	$\sigma_s^{(e)}$	$2.5\,10^{-25}\,\text{m}^2$
Pump background losses	α_p	$3\,10^{-3}\,\text{m}^{-1}$
Signal background losses	α_p	$5\,10^{-3}\,\text{m}^{-1}$
Front mirror reflectivity	$R_s^{(1)}$	0.98
Output mirror reflectivity	$R_s^{(2)}$	0.04
Lifetime of the upper-level atoms	τ	$1.45\,10^{-5}\,\text{s}$
Effective mode area	A_{eff}	$1.39\,10^{-11}\,\text{m}$
Contribution of the spontaneous emission	P_0	$0\,\text{W}$

Table 3: Parameter values for the Tm^{3+} doped fiber-laser investigated in [7].

We have depicted in Fig. 3 the pump and laser powers in the forward and backward directions $P_p^{\pm}, P_s^{\pm}$ as a function of the position along the fiber together with the ratio $N_2(z)/N$. This figure is quite similar to the one depicted in [7, Fig. 5]. Note however that when using the doping substance concentration given in [7] ($N = 4.68\,10^{26}\,\text{ions/m}^3$) rather than the one given in Table 3, the figure we obtain is significantly different from [7, Fig. 5]. We have obtained a forward laser power at $z = 0$ with value $P_s^+(0) = 74.8308$ W and a backward laser power at $z = 0$ with value $P_s^-(0) = 76.358$ W. At the fiber back end $z = L$, the values are $P_s^+(L) = 377.953$ W and $P_s^-(L) = 15.1181$ W. The forward pump power at $z = L$ is 2.02216 W whereas the backward pump power remains zero along the fiber. The CPU time for the simulation was 1.3 s and the error estimator defined in (16b) was $\mathfrak{E}_s = 7.5682\,10^{-12}$.

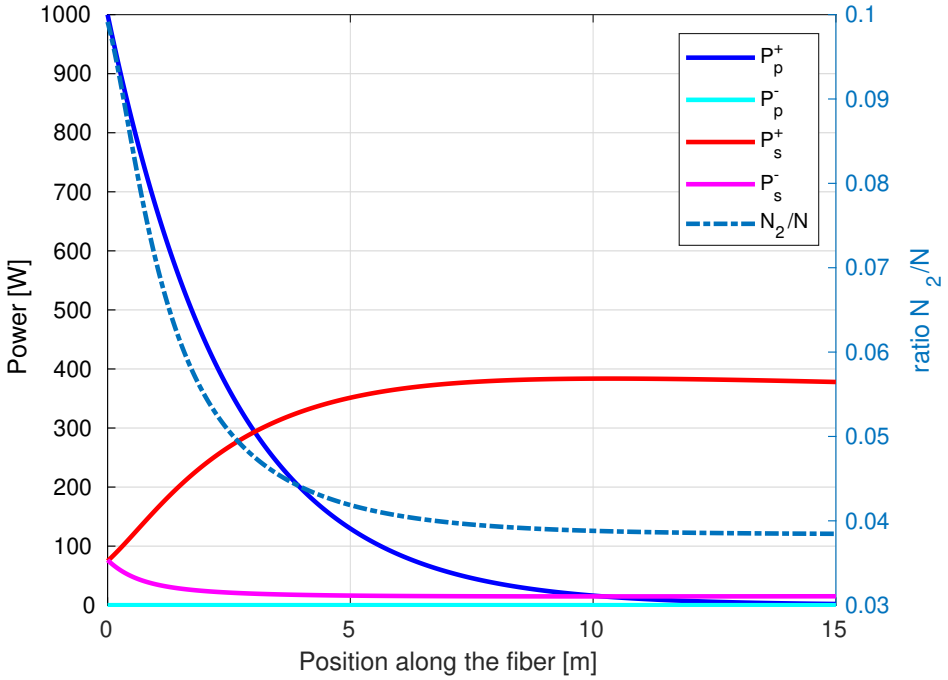

Figure 3: Pump and laser powers in the forward and backward directions $P_p^+, P_p^-, P_s^+, P_s^-$ as a function of the position along the fiber for the Tm^{3+} doped fiber-laser.

4.3 Limitation of the model

We have found some limitations to the model (1) describing light-wave propagation in a high power fiber-laser based on the rate-equation theory under the steady state condition. For the fiber-laser characterized by the parameter values given in Table 4 (fiber IXF-2CF-Yb-O-6-130 from the company iXblue Photonics), the evolution of the pump and laser powers in the forward and backward directions $P_p^{\pm}, P_s^{\pm}$ along the fiber is depicted in Fig. 4. One can observe that the laser signal power in the fiber exceed the pump power injected in the fiber, which is not possible from the physics point of view.

Numerical simulation investigations show that this contradiction can be related to the fact that in this simulation the back end mirror reflectivity is high ($R_s^{(2)} = 20\%$ compared to a value lower than 1% in the simulations shown in Section 4.2) so that a larger part of the signal is reflected back to the fiber. We infer that the mathematical model corresponding to the BVP (6)–(9) is not adequate to describe light-wave propagation in a fiber-laser characterized by the parameter values provided in Table 4.

Parameter	Notation	Value
Fiber length	L	$1\,\mathrm{m}$
Pump wavelength	λ_p	$9.76\,10^{-7}\,\mathrm{m}$
Signal wavelength	λ_s	$1.06\,10^{-6}\,\mathrm{m}$
Pump power launched in the front end	P^+_{pump}	$0.5\,\mathrm{W}$
Pump power launched in the back end	P^-_{pump}	$0\,\mathrm{W}$
Pump overlap factor	Γ_p	0.75
Signal overlap factor	Γ_s	0.75
Doping substance concentration	N_t	$8.5\,10^{24}\,\mathrm{ions/m^3}$
Pump absorption cross section	$\sigma_p^{(a)}$	$2.05\,10^{-24}\,\mathrm{m^2}$
Pump emission cross section	$\sigma_p^{(e)}$	$2.16\,10^{-24}\,\mathrm{m^2}$
Signal absorption cross section	$\sigma_s^{(a)}$	$7.53\,10^{-24}\,\mathrm{m^2}$
Signal emission cross section	$\sigma_s^{(e)}$	$3.62\,10^{-25}\,\mathrm{m^2}$
Pump background losses	α_p	$10^{-2}\,\mathrm{m^{-1}}$
Signal background losses	α_p	$10^{-2}\,\mathrm{m^{-1}}$
Front mirror reflectivity	$R_s^{(1)}$	1
Output mirror reflectivity	$R_s^{(2)}$	0.2
Lifetime of the upper-level atoms	τ	$0.84\,10^{-3}\,\mathrm{s}$
Effective mode area	A_{eff}	$44\,10^{-12}\,\mathrm{m}$
Contribution of the spontaneous emission	P_0	$0\,\mathrm{W}$

Table 4: Parameter values for the fiber-laser

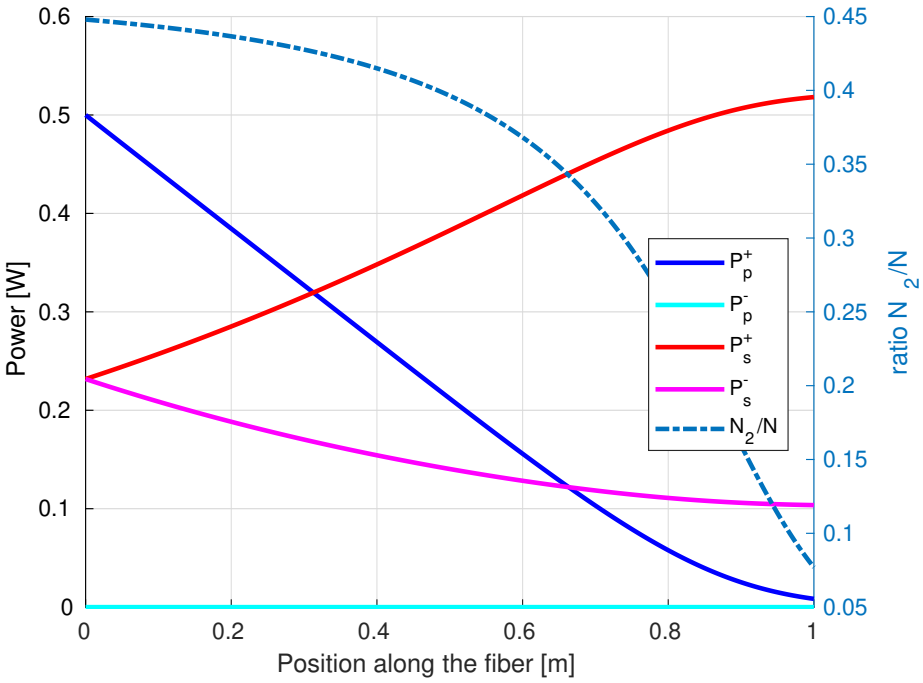

Figure 4: Pump and laser powers in the forward and backward directions $P_p^+, P_p^-, P_s^+, P_s^-$ as a function of the position along the fiber.

Appendix A : An equivalent initial value problem in the absence of losses

We consider in this appendix the special case when the losses and the contribution to spontaneous emission into the propagation laser mode can be neglected. That is to say, we consider BVP (6)–(9) under the assumptions that $\alpha_s = \alpha_p = 0$ and $P_0 = 0$.

In this special case, the solutions $P_p^{\pm}, P_s^{\pm}$ to the set of ODE (6) exhibit the following features: There exist two real numbers C_p and C_s such that for all $z \in [0, L]$

$$P_p^+(z)\, P_p^-(z) = C_p, \qquad P_s^+(z)\, P_s^-(z) = C_s. \tag{A.17}$$

This property can be easily proved by considering the mapping $z \in [0, L] \mapsto P_p^+(z)\, P_p^-(z)$ and showing that its derivative is zero. We have

$$\frac{\mathrm{d}}{\mathrm{d}z}\Big(P_p^+(z)\, P_p^-(z)\Big) = P_p^+(z)\, \frac{\mathrm{d}P_p^-}{\mathrm{d}z}(z) + P_p^-(z)\, \frac{\mathrm{d}P_p^+}{\mathrm{d}z}(z).$$

We then sum equation (6a) for P_p^+ preparatorily multiplied by P_p^- and equation (6a) for P_p^- preparatorily multiplied by P_p^+ to show that the derivative is zero. Note that the properties (A.17) are true even when the losses are not zero. When $P_0 \neq 0$, only the relation on $P_p^{\pm}$ remains valid.

We deduce from (A.17) and from BC (9a) and (9b), the following relationships between the boundary values at the fiber ends:

$$P_p^+(L) = \frac{1}{R_p^{(2)}} \left(\tfrac{1}{4} \big(P_{\mathrm{pump}}^-\big)^2 + R_p^{(1)} R_p^{(2)} \big(P_p^-(0)\big)^2 + P_{\mathrm{pump}}^- R_p^{(2)} P_p^-(0) \right)^{\frac{1}{2}} - \frac{P_{\mathrm{pump}}^-}{2R_p^{(2)}} \tag{A.18a}$$

$$P_s^+(L) = \sqrt{\frac{R_s^{(1)}}{R_s^{(2)}}}\; P_s^-(0) \tag{A.18b}$$

Note that when $R_p^{(2)} = 0$, (A.18a) has to be changed for

$$P_{\mathrm{pump}}^-\, P_p^+(L) = R_p^{(1)} \big(P_p^-(0)\big)^2 + P_{\mathrm{pump}}^+ P_p^-(0). \tag{A.19}$$

Let us now show how we can express the two quantities $P_p^-(0)$ and $P_s^-(0)$ in terms of the known data of the fiber-laser. By difference between (1a) considered for P_p^+ and P_p^- on the one hand and by difference between (1b) considered for P_s^+ and P_s^- on the other hand, one can easily show that N_2 given by (2) can be expressed as

$$N_2(z) = -\frac{\tau_3}{h\, A_{\mathrm{eff}}} \left(\frac{1}{\nu_p} \Big(\frac{\mathrm{d}P_p^+}{\mathrm{d}z}(z) - \frac{\mathrm{d}P_p^-}{\mathrm{d}z}(z) \Big) + \frac{1}{\nu_s} \Big(\frac{\mathrm{d}P_s^+}{\mathrm{d}z}(z) - \frac{\mathrm{d}P_s^-}{\mathrm{d}z}(z) \Big) \right). \tag{A.20}$$

Substituting this expression of N_2 into equations (1a)–(1b), we obtain

$$\begin{cases} \pm \dfrac{\mathrm{d}P_p^{\pm}}{\mathrm{d}z}(z) = -\Big(\dfrac{\mathrm{d}P_p^{\pm}}{\mathrm{d}z}(z) - \dfrac{\mathrm{d}P_p^-}{\mathrm{d}z}(z) \Big) \dfrac{P_p^{\pm}(z)}{P_p^{\mathrm{sat}}} \\ \qquad\qquad - \dfrac{\nu_p}{\nu_s} \Big(\dfrac{\mathrm{d}P_s^{\pm}}{\mathrm{d}z}(z) - \dfrac{\mathrm{d}P_s^-}{\mathrm{d}z}(z) \Big) \dfrac{P_p^{\pm}(z)}{P_p^{\mathrm{sat}}} - \alpha_p^a\, P_p^{\pm}(z) & \text{(A.21a)} \\ \pm \dfrac{\mathrm{d}P_s^{\pm}}{\mathrm{d}z}(z) = -\dfrac{\nu_s}{\nu_p} \Big(\dfrac{\mathrm{d}P_p^{\pm}}{\mathrm{d}z}(z) - \dfrac{\mathrm{d}P_p^-}{\mathrm{d}z}(z) \Big) \dfrac{P_s^{\pm}(z)}{P_s^{\mathrm{sat}}} \\ \qquad\qquad - \Big(\dfrac{\mathrm{d}P_s^{\pm}}{\mathrm{d}z}(z) - \dfrac{\mathrm{d}P_s^-}{\mathrm{d}z}(z) \Big) \dfrac{P_s^{\pm}(z)}{P_s^{\mathrm{sat}}} - \alpha_s^a\, P_s^{\pm}(z) & \text{(A.21b)} \end{cases}$$

Let us consider equation (A.21a) for P_p^+. We divide both side by $P_p^+(z)$ under the assumption that the forward pump power P_p^+ never cancels and we integrate over the interval $[0, L]$:

$$\begin{aligned} \int_0^L \frac{1}{P_p^+(z)} \frac{\mathrm{d}P_p^+(z)}{\mathrm{d}z}\, \mathrm{d}z = &-\frac{1}{P_p^{\mathrm{sat}}} \int_0^L \Big(\frac{\mathrm{d}P_p^+}{\mathrm{d}z}(z) - \frac{\mathrm{d}P_p^-}{\mathrm{d}z}(z) \Big)\, \mathrm{d}z \\ &- \frac{\nu_p}{\nu_s P_p^{\mathrm{sat}}} \int_0^L \Big(\frac{\mathrm{d}P_s^+}{\mathrm{d}z}(z) - \frac{\mathrm{d}P_s^-}{\mathrm{d}z}(z) \Big)\, \mathrm{d}z - \alpha_p^a\, L. \end{aligned}$$

It follows that

$$\log\left(\frac{P_p^+(L)}{P_{\text{pump}}^+ + R_p^{(1)}P_p^-(0)}\right) = -\frac{1}{P_p^{\text{sat}}}\left(P_p^+(L) - P_{\text{pump}}^+ - R_p^{(1)}P_p^-(0) - P_{\text{pump}}^- - R_p^{(2)}P_p^+(L) + P_p^-(0)\right)$$
$$-\frac{\nu_p}{\nu_s P_p^{\text{sat}}}\left(P_s^+(L) - R_s^{(1)}\,P_s^-(0) - R_s^{(2)}\,P_s^+(L) + P_s^-(0)\right) - \alpha_p^a\,L.$$

The same calculation can be done with the three other equations in (A.21a)–(A.21b). Taking into account relations (A.18), it remains the following two equations for the unknowns $P_p^-(0)$ and $P_s^-(0)$:

$$\begin{cases} \log\left(\dfrac{P_{\text{pump}}^+ + R_p^{(1)}P_p^-(0)}{\phi(P_p^-(0))}\right) = \dfrac{\nu_p}{\nu_s}\dfrac{\eta}{P_p^{\text{sat}}}\,P_s^-(0) + \alpha_p^a L + \dfrac{1}{P_p^{\text{sat}}}\Phi(P_p^-(0)) & \text{(A.22a)} \\ \dfrac{1}{2}\log(R_s^{(1)}R_s^{(2)}) = \dfrac{\eta}{P_s^{\text{sat}}}\,P_s^-(0) + \alpha_s^a L + \dfrac{\nu_s}{\nu_p}\dfrac{1}{P_s^{\text{sat}}}\Phi(P_p^-(0)) & \text{(A.22b)} \end{cases}$$

where we have set

$$\eta = \sqrt{\frac{R_s^{(1)}}{R_s^{(2)}} - R_s^{(1)} - \sqrt{R_s^{(1)}R_s^{(2)}} + 1}$$
$$\Phi(P_p^-(0)) = (1-R_p^{(2)})\phi(P_p^-(0)) + (1-R_p^{(1)})P_p^-(0) - (P_{\text{pump}}^+ + P_{\text{pump}}^-)$$
$$\phi(P_p^-(0)) = \sqrt{\left(\frac{P_{\text{pump}}^-}{2R_p^{(2)}}\right)^2 + \frac{R_p^{(1)}}{R_p^{(2)}}\left(P_p^-(0)\right)^2 + \frac{P_{\text{pump}}^-}{R_p^{(2)}}P_p^-(0)} - \frac{P_{\text{pump}}^-}{2R_p^{(2)}}$$

Combining equations (A.22a) and (A.22b), we obtain that

$$\log\left(\frac{P_{\text{pump}}^+ + R_p^{(1)}P_p^-(0)}{\phi(P_p^-(0))}\right) = A \tag{A.23}$$

where

$$A = \frac{\nu_p P_s^{\text{sat}}}{\nu_s P_p^{\text{sat}}}\left(\frac{1}{2}\log(R_s^{(1)}R_s^{(2)}) - \alpha_s^a L\right) + \alpha_p^a L \tag{A.24}$$

From (A.23), we deduce that $P_p^-(0)$ solves the following algebraic equation with unknown X

$$\sqrt{\frac{1}{4}\left(P_{\text{pump}}^-\right)^2 + R_p^{(1)}R_p^{(2)}X^2 + P_{\text{pump}}^- R_p^{(2)}X} - \mathrm{e}^{-A}R_p^{(1)}R_p^{(2)} = \mathrm{e}^{-A}R_p^{(2)}P_{\text{pump}}^+ + \frac{1}{2}P_{\text{pump}}^-.$$

Solving this algebraic equation, we obtain that its non-negative solution reads

$$P_p^-(0) = \frac{P_{\text{pump}}^+ R_p^{(2)} + P_{\text{pump}}^-\,\mathrm{e}^A}{\mathrm{e}^{2A} - R_p^{(1)}R_p^{(2)}} \tag{A.25}$$

Then, form (A.22b) , we have

$$P_s^-(0) = \frac{P_s^{\text{sat}}}{\eta}\left(\frac{1}{2}\log(R_s^{(1)}R_s^{(2)}) - \frac{\nu_s}{\nu_p}\frac{1}{P_s^{\text{sat}}}\Phi(P_p^-(0)) - \alpha_s^a L\right). \tag{A.26}$$

Finally, under the assumption that $\alpha_s = \alpha_p = 0$ and $P_0 = 0$, the BVP (6)–(9) is equivalent to the IVP composed of the ODE (6) and initial conditions (A.25) for $P_p^-(0)$, (A.26) for $P_s^-(0)$, (9a) for $P_p^+(0)$ and (9c) for $P_p^-(0)$.

Note that in [5] the authors also propose an IVP, different of the one proposed here, equivalent to the BVP (6)–(9) under the following additional assumptions: $\sigma_s^{(a)} \ll \sigma_p^{(a)}, \sigma_p^{(e)} = 0$ and $R_p^{(1)} = R_p^{(2)} = 0$. We did not need these additional assumptions here. As well, in [9] the authors proposed an analytical solution to the BVP in the absence of losses but also require additional assumptions.

References

[1] P. Becker, A. Olsson, and J. Simpson, *Erbium-Doped Fiber Amplifiers: Fundamentals and Technology*, Optics and Photonics, Elsevier Science, 1999.

[2] E. Desurvire, *Erbium-Doped Fiber Amplifiers: Principles and Applications*, Wiley Series in Telecommunications and Signal Processing, Wiley, 2002.

[3] X. Hu, T. Ning, L. Pei, Q. Chen, and W. Jian, *Number sequence transition method based on Matlab BVP solvers for high power Yb3+ doped fiber lasers*, Optics & Laser Technology, 58 (2014), pp. 76–83.

[4] X. Hu, T. Ning, L. Pei, Q. Chen, and J. Li, *A simple error control strategy using Matlab BVP solvers for Yb3+ doped fiber lasers*, Optik, 126 (2015), pp. 3446–3451.

[5] I. Kelson and A. A. Hardy, *Strongly pumped fiber lasers*, IEEE Journal of Quantum Electronics, 34 (1998), pp. 1570–1577.

[6] J. Kierzenka and L. F. Shampine, *A BVP solver based on residual control and the Maltab PSE*, ACM Trans. Math. Softw., 27 (2001), pp. 299–316.

[7] J. Liu, C. Zhao, S. Wen, D. Fan, and C. Shuai, *An improved shooting algorithm and its application to high-power fiber lasers*, Optics Communications, 283 (2010), pp. 3764–3767.

[8] MATLAB, *Matlab Documentation (R2018b)*, The MathWorks Inc., available on line at url : https://mathworks.com/help/releases/R2018b, 2018.

[9] M. Peysokhan, E. Mobini, and A. Mafi, *Analytical formulation of a high-power Yb-doped double-cladding fiber laser*, OSA Continuum, 3 (2020), pp. 1940–1951.

[10] L. F. Shampine and M. W. Reichelt, *The Matlab ODE suite*, SIAM Journal on Scientific Computing, 18 (1997), pp. 1–22.

[11] L. Shang, L. Qi, Y. Liao, and S. Zhang, *A combined algorithm for simulating fiber lasers based on the shooting and relaxation methods*, Optical Fiber Technology, 18 (2012), pp. 502–508.